Journal of the American College of Cardiology
© 2014 by the American College of Cardiology Foundation
Published by Elsevier Inc.

Vol. 63, No. 2, 2014
ISSN 0735-1097/$36.00
http://dx.doi.org/10.1016/j.jacc.2013.08.724

CLINICAL RESEARCH | Clinical Trials

Intracoronary Cardiosphere-Derived Cells After Myocardial Infarction

Evidence of Therapeutic Regeneration in the Final 1-Year Results of the CADUCEUS Trial (CArdiosphere-Derived aUtologous stem CElls to reverse ventricULar dySfunction)

Konstantinos Malliaras, MD,* Raj R. Makkar, MD,* Rachel R. Smith, PHD,* Ke Cheng, PHD,* Edwin Wu, MD,† Robert O. Bonow, MD,† Linda Marbán, PHD,* Adam Mendizabal, MS,‡ Eugenio Cingolani, MD,* Peter V. Johnston, MD,§ Gary Gerstenblith, MD,§ Karl H. Schuleri, MD,§ Albert C. Lardo, PHD,§‖ Eduardo Marbán, MD, PHD*

Los Angeles, California; Chicago, Illinois; and Rockville and Baltimore, Maryland

Objectives This study sought to report full 1-year results, detailed magnetic resonance imaging analysis, and determinants of efficacy in the prospective, randomized, controlled CADUCEUS (CArdiosphere-Derived aUtologous stem CElls to reverse ventricULar dySfunction) trial.

Background Cardiosphere-derived cells (CDCs) exerted regenerative effects at 6 months in the CADUCEUS trial. Complete results at the final 1-year endpoint are unknown.

Methods Autologous CDCs (12.5 to 25 $\times$ 10^6) grown from endomyocardial biopsy specimens were infused via the intracoronary route in 17 patients with left ventricular dysfunction 1.5 to 3 months after myocardial infarction (MI) (plus 1 infused off-protocol 14 months post-MI). Eight patients were followed as routine-care control patients.

Results In 13.4 months of follow-up, safety endpoints were equivalent between groups. At 1 year, magnetic resonance imaging revealed that CDC-treated patients had smaller scar size compared with control patients. Scar mass decreased and viable mass increased in CDC-treated patients but not in control patients. The single patient infused 14 months post-MI responded similarly. CDC therapy led to improved regional function of infarcted segments compared with control patients. Scar shrinkage correlated with an increase in viability and with improvement in regional function. Scar reduction correlated with baseline scar size but not with a history of temporally remote MI or time from MI to infusion. The changes in left ventricular ejection fraction in CDC-treated subjects were consistent with the natural relationship between scar size and ejection fraction post-MI.

Conclusions Intracoronary administration of autologous CDCs did not raise significant safety concerns. Preliminary indications of bioactivity include decreased scar size, increased viable myocardium, and improved regional function of infarcted myocardium at 1 year post-treatment. These results, which are consistent with therapeutic regeneration, merit further investigation in future trials. (CArdiosphere-Derived aUtologous stem CElls to reverse ventricULar dySfunction [CADUCEUS]; NCT00893360) (J Am Coll Cardiol 2014;63:110–22) © 2014 by the American College of Cardiology Foundation

From the *Cedars-Sinai Heart Institute, Los Angeles, California; †Division of Cardiology, Department of Medicine, Bluhm Cardiovascular Institute, Northwestern University Feinberg School of Medicine, Northwestern Memorial Hospital, Chicago, Illinois; ‡EMMES Corporation, Rockville, Maryland; §Division of Cardiology, Department of Medicine, The Johns Hopkins University, Baltimore, Maryland; and the ‖Department of Biomedical Engineering, The Johns Hopkins University, Baltimore, Maryland. Funded by U.S. National Heart, Lung, and Blood Institute (U54-HL081028) and Cedars-Sinai Board of Governors Heart Stem Cell Center. Drs. Eduardo Marbán and Linda Marbán are founders and equity holders in Capricor. Dr. Eduardo Marbán is a scientific advisor for Capricor. Drs. Smith and Linda Marbán are employed by Capricor as well as employed part time by the Cedars-Sinai Medical Center. Dr. Malliaras receives consulting fees from Capricor. No one associated with Capricor participated in the recruitment and consent of subjects, in the performance of investigational procedures or in the assessment of adverse events. Capricor provided no funding for this study, nor did the company have approval rights over publications or presentations. All other authors have reported that they have no relationships relevant to the contents of this paper to disclose.

Manuscript received May 1, 2013; revised manuscript received July 21, 2013, accepted August 19, 2013.

Acute myocardial infarction (MI) results in the replacement of living heart muscle by a fibrous scar. Although traditional therapeutic strategies (timely reperfusion and optimal drug- and device-based therapies) have reduced MI-associated mortality (1), new approaches are needed for patients in whom left ventricular (LV) dysfunction develops (2). To that end, over the past decade, cell therapy has emerged as a promising treatment strategy. Multiple cell types including bone marrow mononuclear cells (3–6), bone marrow mesenchymal cells (7), and adipose tissue–derived cells (8) have been used in the setting of acute or convalescent MI, but efficacy has been inconsistent (3–6) and, overall, modest (9). Six-month primary endpoint analysis of the proof-of-concept, prospective, randomized, controlled CADUCEUS (CArdiosphere-Derived aUtologous stem CElls to reverse ventricULar dySfunction) trial (10) demonstrated the feasibility of harvesting, expanding, and delivering autologous CDCs (11) by intracoronary infusion in post-MI patients. We found that autologous CDCs appear to be safe and effective in decreasing scar size, increasing viable myocardium, and improving regional myocardial function at 6 months post-treatment. However, whether these effects are sustained at 1 year after cell administration is unknown. Here, we report the final 1-year endpoint results of the CADUCEUS trial, including a comprehensive magnetic resonance imaging (MRI) analysis of myocardial regeneration and clinical correlates of regenerative efficacy.

Methods

The CADUCEUS study design. The detailed study protocol, complete 6-month (including the primary safety endpoint) and partial 1-year follow-up results of the CADUCEUS trial were reported previously (10,12). In brief, 31 eligible participants with a recent reperfused MI (≤4 weeks previously) and moderate LV dysfunction (ejection fraction [EF] 25% to 45% by clinically indicated post-MI imaging) were randomly allocated in a 2:1 ratio at 2 medical centers in the United States (Cedars-Sinai Medical Center and The Johns Hopkins Hospital) to receive autologous CDCs and standard care or standard care alone. Patients randomized to receive CDCs underwent endomyocardial biopsy to harvest tissue for autologous cell production. When the pre-specified dose was achieved, patients returned for cell infusion using a stop-flow technique via an over-the-wire balloon angioplasty catheter, positioned in the infarct-related coronary artery at the site of the previously implanted stent. One patient petitioned to undergo late treatment and was infused 14 months post-MI, after a protocol exception was approved by the U.S. Food and Drug Administration and by the Cedars-Sinai institutional review board.

Patients were followed 2 weeks and 1, 2, 3, 6, and 12 months after CDC infusion or at corresponding comparable times post-MI for control patients. Patients underwent 48-h ambulatory electrocardiographic monitoring at each study visit. Adverse events were independently monitored by a physician at the Data Coordinating Center (EMMES Corporation, Rockville, Maryland) and by the National Heart, Lung, and Blood Institute Gene and Cell Therapy Data and Safety Monitoring Board (DSMB). Efficacy was assessed by the New York Heart Association (NYHA) functional class, the Minnesota Living With Heart Failure Questionnaire (13), the 6-min walk test (6MWT), peak oxygen consumption (Vo_2), and MRI. Contrast-enhanced cardiac MRI studies were performed at baseline and at 6 and 12 months.

Cardiac MRI in the CADUCEUS trial. Cardiac MRI was performed to measure LV scar mass, LV viable myocardial mass (i.e., total LV mass minus LV scar mass), scar size (LV scar mass divided by total LV mass), LV volumes, global function, and regional function. MRI was performed using 1.5-T magnets (Avanto, Siemens Medical Solutions, Erlangen, Germany). Global LV function, regional systolic thickening, and regional end-systolic thickness were assessed using a true fast imaging steady-state free-precession pulse sequence (TrueFISP) with breath-holding acquisitions (14). LV endo- and epicardial borders, defined in the end-diastolic and end-systolic frame in contiguous slices, were used to calculate LV parameters (LV end-diastolic and end-systolic volumes, LV mass, EF) as described (15), using U.S. Food and Drug Administration–approved software (QMass MR, Medis Medical Imaging Systems, Leiden, the Netherlands). To measure regional systolic thickening and end-systolic thickness in infarcted myocardial segments, each cardiac short-axis slice was divided into 6 segments, using the right ventricular insertion as a reference point. Infarcted myocardial segments were visually identified from matched delayed contrast-enhanced images, and systolic thickening and end-systolic thickness were calculated for each infarcted segment (QMass MR, Medis Medical Imaging Systems). To assess circumferential strain, cardiac magnetic resonance tagged images were acquired with an electrocardiographically gated, segmented K-space, fast gradient-recalled-echo pulse sequence with spatial modulation of magnetization to generate a grid-tagged pattern (16). Tagged images were quantitatively analyzed using a custom software package (Diagnosoft HARP, Diagnosoft Inc., Palo Alto, California), as described

Abbreviations and Acronyms

- **CDC** = cardiosphere-derived cell
- **CK-MB** = creatine kinase-myocardial band
- **CT** = computed tomography
- **DSMB** = Data and Safety Monitoring Board
- **Ecc** = systolic circumferential strain
- **EDV** = end-diastolic volume
- **EF** = ejection fraction
- **ESV** = end-systolic volume
- **FWHM** = full width at half maximum
- **ICD** = implantable cardioverter-defibrillator
- **LV** = left ventricular
- **LVEF** = left ventricular ejection fraction
- **MI** = myocardial infarction
- **MRI** = magnetic resonance imaging
- **NYHA** = New York Heart Association
- **SAE** = serious adverse event(s)
- **TnI** = troponin I
- **Vo_2** = oxygen consumption

JACC Vol. 63, No. 2, 2014
January 21, 2014:110–22

previously (17). The peak systolic circumferential strain (Ecc), determined from the strain map of each point, was assessed in infarcted segments. The American Heart Association 16-segment model (18) was used, and infarcted segments were visually identified (from delayed contrast-enhanced images) in 3 short-axis slices (1 basal slice, 1 mid-ventricular, and 1 apical slice for each patient). Mid-wall Ecc, a measure of regional contractility calculated from tagged cardiac magnetic resonance images (19), was assessed in each infarcted segment. Approximately 15 min after intravenous delivery of gadolinium diethylenetriamine pentaacetic acid contrast (0.2 mmol/kg body weight, Magnevist, Berlex, Wayne, New Jersey), delayed contrast-enhanced images were acquired to assess scar size with an electrocardiographically gated, breath-hold, interleaved, inversion recovery, 2-dimensional TurboFLASH sequence (20). Scar size from delayed contrast-enhanced cardiac MRI was defined based on the full width at half maximum (FWHM) criterion (21), which uses pixels with >50% of the maximal signal intensity to delineate scarred myocardium. For the parameters specified above, images were analyzed in the core laboratory at The Johns Hopkins University by an experienced observer blinded to treatment groups (QMass MR, Medis Medical Imaging Systems). Delayed contrast-enhanced images obtained from 2 CDC-treated patients were deemed technically uninterpretable by the imaging core laboratory and were excluded from analysis. Additional comprehensive analysis of myocardial regeneration was carried out by a reader at the Cedars-Sinai Heart Institute (K.M.), using the infarct contours determined by The Johns Hopkins University imaging core laboratory. Delayed contrast-enhanced images and their corresponding cine short-axis cardiac images were matched across time points (baseline and 1 year). Each cardiac slice was divided into 6 segments (using the right ventricular insertion as a reference point), infarcted segments were visually identified from delayed contrast-enhanced images, and scar size and systolic thickening were calculated for each individual infarcted segment at baseline and 1 year.

Three patients received implantable cardioverter-defibrillators (ICDs) due to clinical indications (low EF) during the course of the study; a contraindication to MRI developed in these patients, and therefore they underwent cardiac computed tomography (CT) instead. Two patients had ICDs implanted between the 6-month and 1-year visits; as a result, these patients underwent MRI at screening, baseline, and 6 months and CT imaging at 1 year. One patient had the ICD implanted between screening and baseline; as a result, this patient underwent MRI at screening and CT at baseline, 6 months, and 1 year. Validation studies comparing MRI with CT have shown that, although changes in scar size, global function, and volumes are comparable when the same modality (either MRI or CT) is used across time points, CT and MRI values cannot be used interchangeably (especially for infarct size measurements) (15); we therefore chose not to mix different imaging modalities in the present analyses. Thus, within-patient treatment effects presented in the main paper were calculated only for data collected with matching modalities; MRI was used in all cases except for the single study patient who underwent CT at baseline, 6 months, and 1 year. The results from this patient were representative of CDC-treated patients; omission of the imaging data from that patient did not influence any of the conclusions. For the sake of inclusiveness, all collected measurements are presented in the Online Appendix, regardless of whether data were obtained with matching (MRI-MRI, CT-CT) or nonmatching (MRI-CT) imaging modalities at different time points; however, the nonmatching data should be interpreted cautiously given the intrinsic differences between MRI and CT as means of quantifying scar (15).

Based on the above, the within-patient treatment effects of EF, EDV, ESV, cardiac output, stroke volume, and LV mass (between baseline and 1 year) presented in the paper come from 14 CDC-treated patients (17 patients minus 1 who was lost to follow-up and 2 who were switched from MRI to CT and thus did not have data from matching imaging modalities) and 7 control patients (8 control patients, 1 of whom was lost to follow-up). The absolute values of EF, EDV, ESV, cardiac output, stroke volume, and LV mass presented in the paper come from 13 CDC-treated patients (as we chose not mix absolute values obtained from MRI and CT, and thus we excluded the 1 patient who underwent CT at baseline and 1 year) and 7 control patients. The within-patient treatment effects of scar size, scar mass, and viable mass (between baseline and 1 year) presented in the paper come from 12 CDC-treated patients (as these parameters are calculated from delayed contrast-enhanced images and delayed contrast-enhanced images obtained from 2 CDC-treated patients were deemed technically uninterpretable by the imaging core laboratory) and 7 control patients. The absolute values of scar size, scar mass, and viable mass presented in the paper come from 11 CDC-treated patients (as we chose not to mix absolute values obtained from MRI and CT, and thus we excluded the 1 patient who underwent CT at baseline and 1 year) and 7 control patients.

Relationship between scar size and EF in convalescent MI patients. To investigate the relationship between scar size and EF in convalescent MI patients, 90 patients underwent cardiac MRI ~5 months after MI (days from MI to MRI: 156 ± 107) at Northwestern Memorial Hospital. Cardiac MRI was performed using a 1.5-T clinical scanner (Sonata or Avanto, Siemens). All images were acquired during repeated breath-holds and were electrocardiographically gated (22). Global LV function was assessed using a cine steady-state free-precession sequence. Delayed contrast-enhanced images were acquired to assess scar size 10 min after the intravenous delivery of gadolinium contrast (0.2 mmol/kg body weight) using a T1-weighted, inversion recovery, fast gradient-echo pulse sequence (20). Left

ventricular ejection fraction (LVEF) and scar size were measured by a blinded expert observer as described (22).

Statistics. Results are presented as mean ± SD in the text and tables and as mean ± SEM in the figures. Categorical data were tested using Fisher's exact test. For continuous measures, normality of data in each group was tested using the Shapiro-Wilk test. If normality was established, differences between 2 groups (control patients and CDC-treated patients) were tested using an independent-sample Student *t* test. If normality could not be established, differences between the 2 groups were tested using the nonparametric Mann-Whitney *U* test. Comparisons of changes from baseline within groups were performed using a paired Student *t* test (if normality was established) or the nonparametric Wilcoxon test (if normality could not be established). Repeated-measures analyses (when >2 time points were included in the analysis [troponin I (TnI)] and creatine kinase-myocardial band [CK-MB]) were performed using the Friedman test; post-hoc analysis was conducted with the Wilcoxon signed rank test with Bonferroni correction (to adjust for multiple comparisons). To investigate predictors of regenerative efficacy, bivariate Pearson's correlation and multiple linear regression analyses were performed. It should be noted that there is no reasonable expectation of a *linear* correlation between parameters, but the regressions are presented to indicate trends other than zero. No multiplicity adjustment for multiple efficacy endpoints was performed because these endpoints were exploratory and hypothesis generating. All tests were 2 sided, and a p value < 0.05 was considered statistically significant. The results of the Shapiro-Wilk test, the test used for between-groups or within-group comparisons, and the calculated p values for all statistical comparisons included in the paper are listed in the Online Appendix.

Results

Patient population and CDC characteristics. A total of 31 patients were randomized (23 to the CDC group and 8 to the control group). Of the 23 patients allocated to the CDC group, 2 withdrew consent before biopsy specimen procurement, 1 became ineligible for infusion due to an occlusion of the infarct-related artery detected incidentally at the time of intended infusion, and there were 3 technical manufacturing failures (for details, see elsewhere [10]). Thus, the final patient population consisted of 17 CDC-treated patients and 8 control patients. Four patients received a low dose of 12.5 million CDCs, 12 received a higher dose of 25M CDCs (defined as the maximal safe dose in pre-clinical studies [23]) and 1 received an intermediate dose of CDCs (17.3 million) to fit within the protocol-specified constraint of the delivery window (no longer than 90 days post-MI). The required CDC dose was achieved at an average of 36 ± 6 days after biopsy procurement and 65 ± 14 days post-MI. Two patients (1 treated and 1 control) were lost to follow-up and did not complete their 1 year visits. One patient, who was randomized to the CDC group underwent biopsy but did not receive CDCs due to a technical manufacturing failure, completed all follow-up studies during the first year (including cardiac MRI) and subsequently underwent a repeat biopsy and infusion off-protocol 14 months post-MI. This patient was followed for 1 additional year post-CDC infusion and underwent additional cardiac MRI studies at 6 months and 1 year post-CDC infusion (20 and 26 months post-MI, respectively).

There were no significant differences in baseline characteristics between groups (a detailed list of baseline characteristics is available elsewhere [10]). The left anterior descending coronary artery (or its diagonal branch) was the culprit vessel of the index MI in 92% of the patients. The average LVEF at baseline was 39 ± 12%, the average scar size equaled 24 ± 10%, and 74% of patients were NYHA functional class I.

Consistent with previous characterizations (11,24), flow cytometry revealed that CDCs are cells of nonhematological origin ($CD45^-$) that are uniformly positive for CD105; 25.1% of CDCs were positive for CD90 (a marker of mesenchymal cells [25,26] or fibroblasts [27]), 2.9% were positive for c-Kit (associated with a subtype of cardiac progenitors [28]), whereas <4% of CDCs were positive for fibroblast (discoidin domain-containing receptor 2 [29]), myofibroblast (α-smooth muscle actin [30]), smooth muscle cell (α-smooth muscle actin), or endothelial cell (CD31) markers (31) (Fig. 1).

Safety. No serious adverse events (SAEs) were associated with biopsy procurement. CDCs are known to be large relative to capillaries (~20-μm vs. ~8-μm diameter), so that microvascular occlusion is expected as the dose escalates (23,32). We thus looked carefully for any evidence of clinically significant infusion-related MI or of subclinical increases in ischemic biomarkers in CDC-treated patients. On average, TnI (but not CK-MB) increased significantly, from a mean of 0.048 ng/ml to a peak of 0.157 ng/ml at 24 h, with full resolution at 14 days (0.044 ng/ml) ($p < 0.001$). Among individual patients, 15 had no increase in TnI (as ruled by the DSMB), whereas 2 experienced mild discrete elevations judged to be related to treatment. An additional patient experienced ST-segment elevations with chest pain during the balloon occlusion for infusion, which resolved fully afterward, without changes in TnI. A complete list of the acquired TnI and CK-MB data for each CDC-treated patient is provided in Online Table 1.

Within 12 months of infusion, SAEs (classified according to MedDRA) were noted in 7 patients: 6 of 17 (35.3%) CDC-treated and 1 of 8 (12.5%) control patients ($p = 0.36$). The 8 episodes of SAEs experienced in the CDC group by 12 months included acute MI ($n = 1$), chest pain ($n = 2$), coronary revascularization ($n = 1$), ICD insertion ($n = 1$), and other 3 noncardiac events (dyspepsia, anxiety, alcohol poisoning). Two of the 8 SAEs (chest pain and ICD

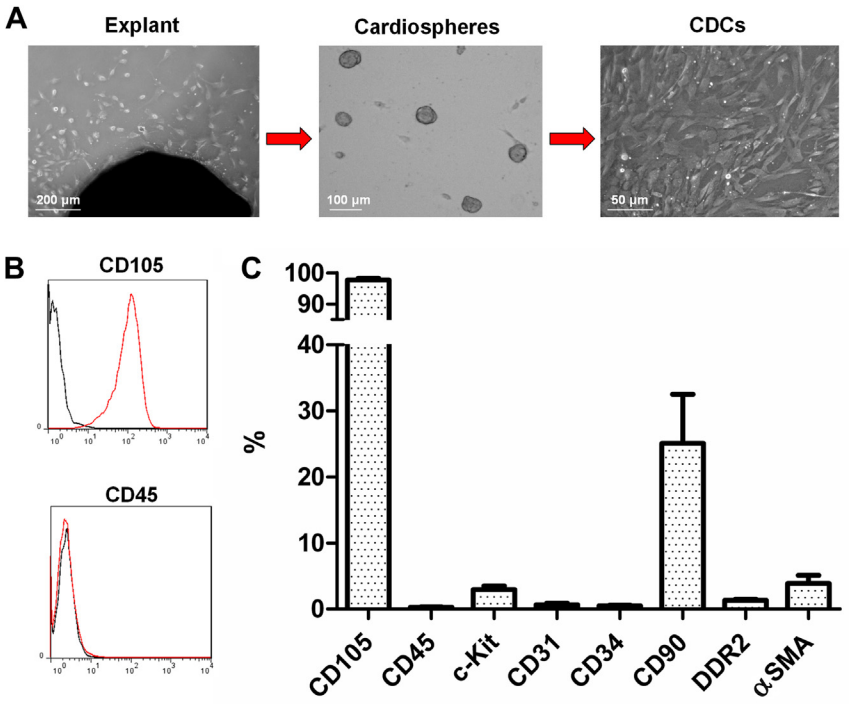

Figure 1 CDC Manufacturing and Phenotypic Characterization

(A) Biopsy specimens are minced into ~1 mm^3 explants. Explants are plated and spontaneously yield outgrowth cells **(left)**. Outgrowth cells are harvested and plated in suspension culture, where they self-assemble into cardiospheres **(middle)**. Cardiospheres are subsequently replated in fibronectin-coated dishes to yield CDCs **(right)**. **(B)** Representative flow cytometry histograms for CD105 and CD45. **(C)** Antigenic profile of CDCs by flow cytometry. CDC = cardiosphere-derived cell; DDR2 = discoidin domain-containing receptor 2; SMA = smooth muscle actin.

insertion) occurred after randomization but before CDC infusion. Two episodes of SAEs occurred in the control group (in 1 patient): chest pain (n = 1) and a noncardiac event (hiatal hernia [n = 1]). The only SAE ruled by the DSMB to be possibly related to the study therapy was a non–ST-segment elevation MI in 1 CDC-treated patient occurring 7 months after cell infusion. During serial follow-up Holter recordings, 8 of 17 (47.1%) CDC-treated patients and 2 of 8 (25%) controls had at least 1 episode of ventricular tachycardia (defined as 3 consecutive beats at a rate ≥100 beats/min, p = 0.4 between groups). All episodes were asymptomatic and brief in duration; the average duration did not differ significantly between groups (4.0 ± 2.2 beats/min [CDCs] vs. 4.0 ± 1.4 beats/min [controls], p = 0.655). No episodes of sustained ventricular tachycardia or ventricular fibrillation were recorded during follow-up. By 12 months, 6 patients in the CDC group reported a hospitalization (8 hospitalization events), whereas 1 control patient did so (2 hospitalization events) (p = 0.36). Two of 8 hospitalizations in the CDC group occurred after randomization but before CDC infusion. Apart from the aforementioned non–ST-segment-elevation MI, no events were noted when considering death, major adverse cardiac events (composite of death and hospital admission for heart failure or nonfatal recurrent MI), or tumor formation seen on MRI (Table 1). With regard to the 2 patients (1 treated and 1 control) who were lost to follow-up and did not complete their 1-year visits, we have ascertained from the Social Security Death Index (33) that both patients were alive at the 1-year endpoint; however, we have no other information on them.

Efficacy: functional and quality-of-life assessments. NYHA functional class did not change significantly between baseline and 1 year in either the treated or the control group (baseline: NYHA functional class I [12 of 16 vs. 6 of 8], NYHA functional class II [4 of 16 vs. 1 of 8], NYHA functional class III [0 of 16 vs. 1 of 8]; 1 year: NYHA

Table 1 Adverse Events in CDC-Treated and Control Patients

	CDCs	Controls	p Value
Serious adverse events	6/17	1/8	0.36
Hospitalizations	6/17	1/8	0.36
Nonsustained ventricular tachycardia	8/17	2/8	0.40
Sustained ventricular tachycardia/ventricular fibrillation	0/17	0/8	1.0
Death/MACE/tumor	1/17	0/8	1.0

CDC = cardiosphere-derived cell; MACE = major adverse cardiac event(s).

Table 2 Pooled Data of MRI-Measured Parameters in CDC-Treated and Control Patients

	CDCs	Controls	p Value
Scar mass at baseline, g	26.6 ± 11.5	23.3 ± 5.5	0.482
Scar mass at 1 yr, g	16.2 ± 8.1	21.6 ± 7.1	0.167
Δ Scar mass, g	−11.9 ± 6.8	−1.7 ± 7.8	0.008
Scar size at baseline, % LV	23.8 ± 9.9	22.4 ± 7.9	0.768
Scar size at 1 yr, % LV	12.9 ± 6.1	20.3 ± 7.5	0.036
Δ Scar size, % LV	−11.1 ± 4.6	−2.2 ± 7.1	0.004
Viable mass at baseline, g	86.9 ± 24.5	85.0 ± 23.8	0.874
Viable mass at 1 yr, g	108.3 ± 24.8	86.8 ± 19.4	0.070
Δ Viable mass, g	22.6 ± 9.4	1.8 ± 8.7	<0.001
EDV at baseline, ml	169.5 ± 40.1	151.7 ± 34.7	0.338
EDV at 1 yr, ml	156.9 ± 57.3	151.6 ± 47.4	0.838
Δ EDV, ml	−12.7 ± 56.0	−0.2 ± 26.1	0.636
ESV at baseline, ml	97.8 ± 34.4	91.4 ± 32.1	0.938
ESV at 1 yr, ml	84.3 ± 43.1	82.5 ± 37.3	0.817
Δ ESV, ml	−13.2 ± 48.1	−8.9 ± 18.7	0.913
EF at baseline, %	42.4 ± 8.9	42.5 ± 11.1	0.987
EF at 1 yr, %	48.2 ± 10.3	48.2 ± 11.4	0.997
Δ EF, %	5.4 ± 10.6	5.8 ± 3.3	0.636
Stroke volume at baseline, ml	71.7 ± 19.2	60.3 ± 9.9	0.162
Stroke volume at 1 yr, ml	72.6 ± 23.9	69.1 ± 18.2	0.757
Δ Stroke volume, ml	0.5 ± 10.1	8.8 ± 9.9	0.090
Cardiac output at baseline, l/min	4.7 ± 1.4	4.0 ± 0.8	0.261
Cardiac output at 1 yr, l/min	4.4 ± 1.3	4.4 ± 1.2	0.926
Δ Cardiac output, l/min	−0.4 ± 1.3	0.4 ± 0.6	0.194
Left ventricular mass at baseline, g	114.9 ± 24.7	108.2 ± 24.1	0.567
Left ventricular mass at 1 yr, g	121.3 ± 25.5	108.3 ± 19.9	0.260
Δ Left ventricular mass, g	6.5 ± 13.5	0.1 ± 7.4	0.079

Values are mean ± SD.

CDC = cardiosphere-derived cell; EDV = end-diastolic volume; EF = ejection fraction; ESV = end-systolic volume; LV = left ventricle; MRI = magnetic resonance imaging.

functional class I [14 of 16 vs. 6 of 7], NYHA functional class II [2 of 16 vs. 1 of 7], NYHA functional class III [0 of 16 vs. 0 of 7] in the treated and control groups, respectively). At 1 year, peak V_{O_2} remained unchanged in both the treated (baseline: 29.2 ± 5.2 ml/kg/min, 1 year: 31.4 ± 6.9 ml/kg/min; p = 0.121) and control groups (baseline: 33.1 ± 6.2 ml/kg/min, 1 year: 37.2 ± 4.7 ml/kg/min; p = 0.192). No change was observed in the total Minnesota Living With Heart Failure Questionnaire score in either the treated (baseline: 21.9 ± 14.9, 1 year: 20.5 ± 20.8; p = 0.649) or the control group (baseline: 32.7 ± 24.8, 1 year: 20.7 ± 21.0; p = 0.100). Patients who received CDCs showed a trend toward an increase in distance walked in 6 min at 1 year (461.1 ± 128.5 m) compared with baseline (baseline: 433.2 ± 115.4; p = 0.086) that was not observed in control patients (baseline: 439.3 ± 75.2m, 1 year: 429.7 ± 61.3 m; p = 0.786).

Efficacy: cardiac MRI. We used cardiac MRI to look for potential indicators of regenerative or functional efficacy. The pooled data of MRI-measured parameters are presented in Table 2, and a complete list of all MRI-measured parameters for each patient is provided in Online Table 2.

The pooled absolute changes in scar size (scar mass normalized by total LV mass) from baseline to 1 year are presented in Figure 2A. Scar size remained unchanged in controls (Δ = −2.2 ± 7.1%, p = 0.452 within group) but decreased in CDC-treated patients (Δ: −11.1 ± 4.6%, p < 0.001 within group, p = 0.004 between groups) over the period of 1 year (Fig. 2A, Online Fig. 1A). The absolute decrease in scar size observed in CDC-treated patients amounted to a 45.4% (± 12.5%) relative decrease in scar size and resulted in significantly smaller scar size in CDC-treated patients (12.9 ± 6.1%) compared with controls (20.3 ± 7.5%, p = 0.036 between groups) 1 year after cell infusion.

Cardiac MRI can quantify independently scar mass and viable mass (the 2 variables that determine scar size). Both scar mass (Δ = −1.7 ± 7.8 g, p = 0.588 within group) and viable mass (Δ = +1.8 ± 8.7 g, p = 0.605 within group) remained virtually unchanged in control patients over 1 year. In contrast, CDC-treated patients exhibited sizable decreases in scar mass (−11.9 ± 6.8 g, p < 0.001 within group, p = 0.008 between groups) and increases in viable mass (+22.6 ± 9.4 g, p < 0.001 within group, p < 0.001 between groups) over the period of 1 year after cell infusion (Fig. 2B, Online Figs. 1B and 1C). Importantly, the observed reductions in scar mass correlated with the increments in viable myocardium, consistent with a therapeutic response in which scar is replaced by viable myocardium (Fig. 2C, Online Fig. 1D).

Online Figure 2 shows the MRI measurements of scar size, scar mass, and viable mass in the single patient who was infused with CDCs 14 months post-MI. This patient responded in a manner qualitatively similar to that of patients treated 1.5 to 3 months post-MI: scar size decreased by 7.2%, scar mass decreased by 5.8 g, and viable mass increased by 14.3 g over the year after CDC infusion; the aforementioned parameters had not improved spontaneously during the first 14 months post-MI.

Regional function was assessed in infarcted myocardial segments (defined as segments containing scar at baseline), after visual identification of such segments in corresponding delayed contrast-enhanced images. At baseline, regional function of infarcted segments (as measured by mid-wall Ecc, systolic thickening, and end-systolic thickness) was similar between groups. At 1 year, CDC-treated infarcted myocardial segments displayed improved (more negative) mid-wall Ecc (−12.7 ± 5.9% vs. −10.0 ± 4.5%, p = 0.020 between groups), increased systolic thickening (35.9 ± 31.8% vs. 28.4 ± 22.4%, p = 0.008 between groups), and increased end-systolic thickness (10.3 ± 3.2 mm vs. 9.4 ± 3.7 mm, p = 0.004 between groups) compared with infarcted segments of control patients (Figs. 2D to 2F).

To determine whether the improvement in regional function correlates with the increase in regional tissue viability, we matched delayed contrast-enhanced images and

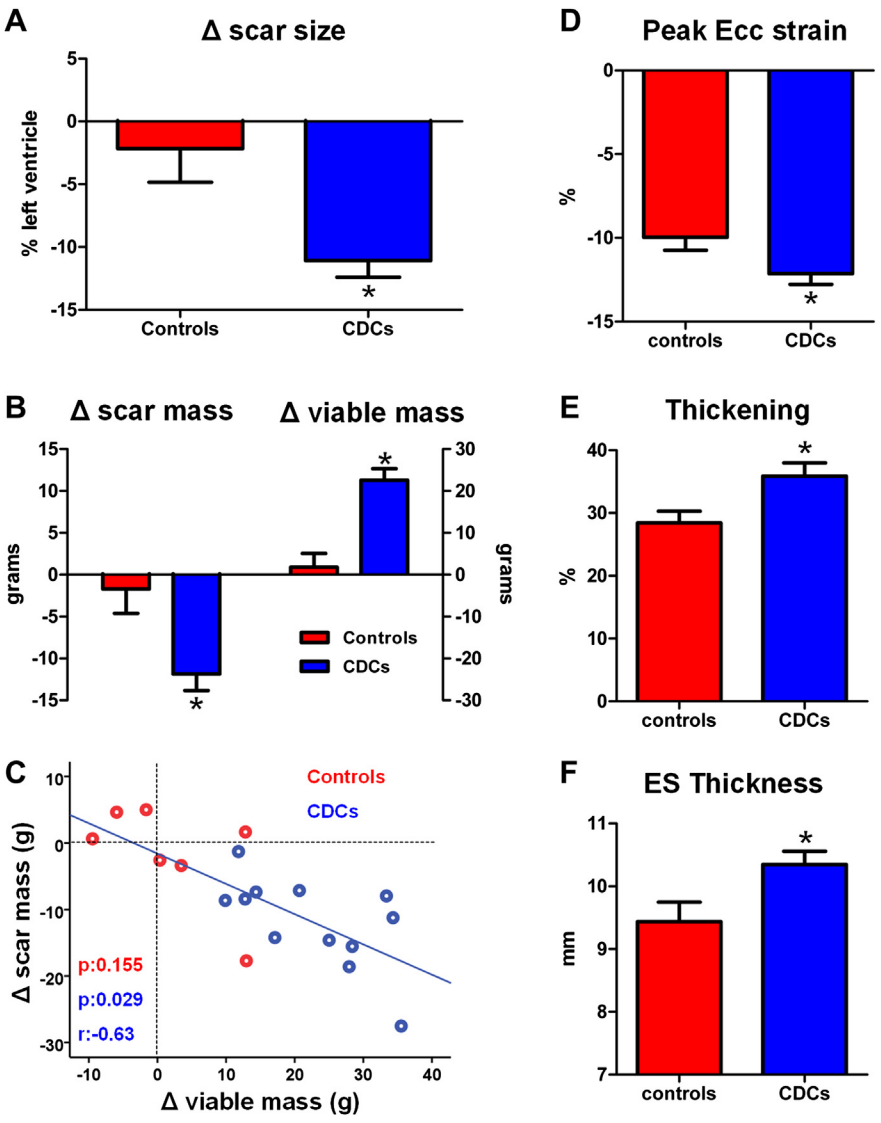

Figure 2 **Autologous CDCs Decrease Scar Size, Decrease Scar Mass, Increase Viable Myocardium, and Improve Regional Function of Infarcted Myocardium**

(A) Changes in scar size from baseline to 1 year. **(B)** Changes in scar mass and viable mass from baseline 1 year. **(C)** Correlation between the change in scar mass and the change in viable mass in individual control and CDC-treated subjects from baseline to 1 year (blue line of best fit is derived only from the CDC-treated patients). **(D)** Regional strain in infarcted segments at 1 year in control patients and CDC-treated patients. **(E)** Systolic thickening in infarcted segments at 1 year in control and CDC-treated patients. **(F)** End-systolic thickness in infarcted segments at 1 year in controls and CDC-treated subjects. *$p < 0.05$ compared to controls. CDC = cardiosphere-derived cell; Ecc = systolic circumferential strain; ES = end-systolic.

their corresponding cine short-axis images across time points (baseline and 1 year) and investigated whether changes in the percentage of infarcted tissue correlate (inversely) with changes in regional systolic function (measured by systolic thickening). Figure 3A shows representative examples of this analysis. At baseline, the delayed contrast-enhanced images in both patients show an anteroseptal scar (of approximately the same size, pseudocolored in pink as determined by the semiautomated FWHM analysis) that is accompanied by a similar degree of hypokinesia in the infarcted myocardial segments. One year later, in the control patient, there are no major changes in scar mass, viable myocardial mass, or regional systolic function. In contrast, in the treated patient, the scar decreased in both circumference and transmurality, whereas viable myocardial mass increased 1 year after CDC infusion. The treated infarcted segments (highlighted by arrows) showed a recovery of systolic function over the period of 1 year (Fig. 3A; see also Online Videos 1, 2, 3, and 4). Figure 3B shows scatterplots of the changes in the percentage of infarcted tissue and the changes in systolic thickening for every infarcted segment of treated and control patients. The infarcted segments of the control patients on

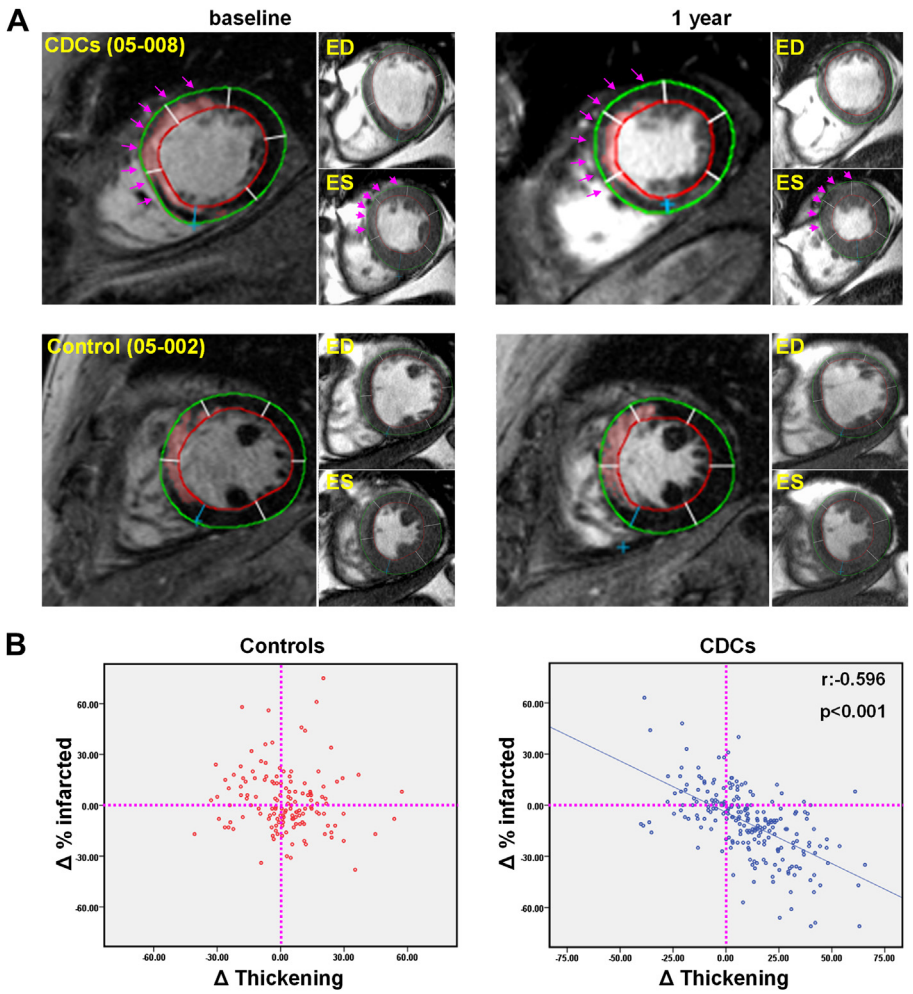

Figure 3 **Comprehensive Magnetic Resonance Imaging Analysis of Regeneration**

(A) Representative matched, delayed contrast-enhanced magnetic resonance images and their corresponding cine short-axis images (at end-diastole [ED] and end-systole [ES]) at baseline and 1 year (see Online Videos 1, 2, 3, and 4). In the pseudocolored, delayed contrast-enhanced images, infarct scar tissue, as determined by the full width half maximum method, appears pink. Each cardiac slice was divided into 6 segments (using the right ventricle insertion as a reference point). Infarcted segments were visually identified from delayed contrast-enhanced images. Scar size (percentage of infarcted tissue per segment) and systolic thickening were calculated for each individual infarcted segment at baseline and 1 year. Endocardial **(red)** and epicardial **(green)** contours of the left ventricle are shown. In the CDC-treated patient **(top row)**, scar decreased, viable mass increased and regional systolic function improved over the period of 1 year in the treated infarcted segments **(highlighted by arrows)**. In contrast, no major changes in scar mass, viable myocardial mass, or regional systolic function were observed in the control patient **(bottom row)**. **(B)** Scatterplots of the changes in the percentage of infarcted tissue and the changes in systolic thickening for every infarcted segment of treated and control patients. ED = end-diastole; other abbreviations as in Figures 1 and 2.

average exhibited no change in either the percentage of infarcted tissue or systolic thickening over time; no correlation was evident between the 2 parameters ($p = 0.277$). In contrast, a substantial portion of the CDC-treated infarcted segments showed a decrease in the percentage of scar tissue coupled with an improvement of systolic thickening over 1 year. The decrease in the percentage of infarcted tissue correlated strongly with the improvement in systolic function ($r = -0.596$, $p < 0.001$).

In terms of global LV function, no differences in the change of LVEF from baseline to 1 year were observed between CDC-treated patients (5.4 ± 10.6%) and control patients (5.8 ± 3.3%, $p = 0.636$ between groups). To investigate whether the changes in LVEF in CDC-treated patients are consistent with the observed reductions in scar size and whether the changes in control subjects fall within the range of expected variability, we examined the natural relationship between scar size and EF in convalescent MI independent of cell therapy. As previously described (22), 90 patients underwent cardiac MRI post-MI for measurement of EF and scar size. The previously unpublished results at ~5 months post-MI (a time at which scar size has stabilized) are depicted in the scatterplot in Figure 4. When the mean values for scar size and EF in CADUCEUS patients are superimposed onto the scatterplot, it becomes evident that the changes in LVEF in CDC-treated patients

JACC Vol. 63, No. 2, 2014
January 21, 2014:110–22

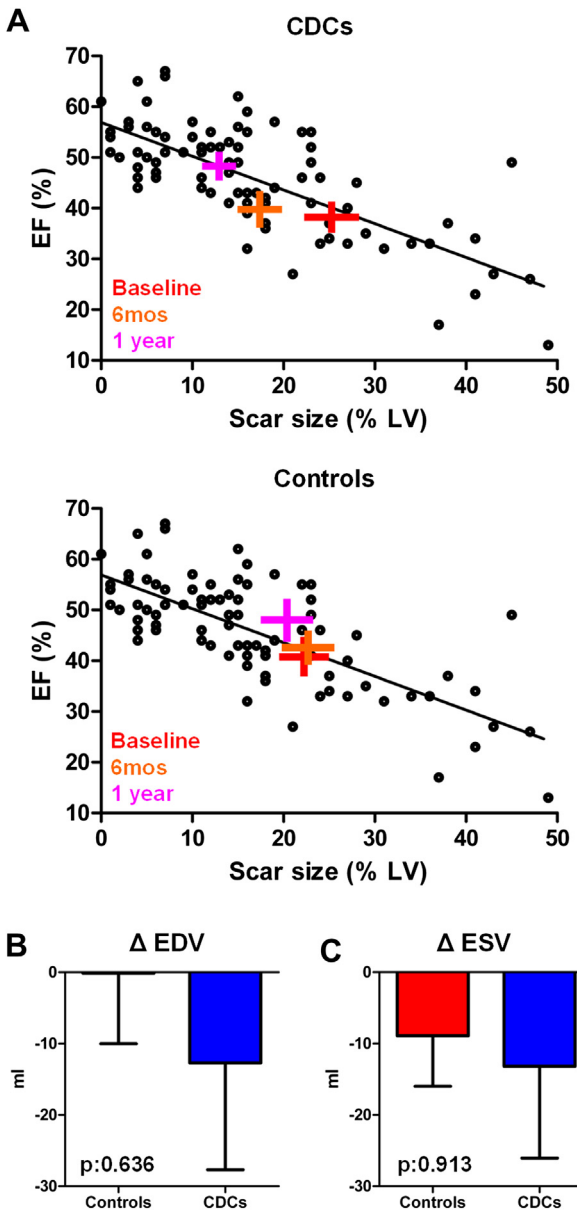

Figure 4 Global Function and Left Ventricular Volumes

(A) Scatterplot showing the natural relationship between scar size and left ventricular ejection fraction ~5 months post-myocardial infarction **(circles)**. Each cross symbol represents the mean values (at the intersection of the vertical and horizontal bars [obtained from all patients with magnetic resonance imaging measurements]), whereas the width of each bar equals ±SEM of scar size and left ventricular ejection fraction of CADUCEUS patients at baseline, 6 months, and 1 year; the crosses are superimposed onto the scatterplot showing prior data from post-myocardial infarction patients with variable scar sizes. The changes in left ventricular ejection fraction in CDC-treated subjects are consistent with the natural relationship between scar size and ejection fraction in convalescent myocardial infarction, whereas the changes in left ventricular ejection fraction in controls fall within the margins of variability. **(B)** Changes in end-diastolic volume from baseline to 1 year. **(C)** Changes in end-systolic volume from baseline to 1 year. CDCs = cardiosphere-derived cells; EDV = end-diastolic volume; EF = ejection fraction; ESV = end-systolic volume; LV = left ventricle.

are consistent with the natural relationship between scar size and EF in convalescent MI, whereas the changes in LVEF in control patients fall within the margins of variability (Fig. 4A, Online Fig. 3). With regard to cardiac volumes, no differences in the change of end-diastolic (Fig. 4B) and end-systolic (Fig. 4C) volumes from baseline to 1 year were seen in CDC-treated patients ($\Delta EDV = -12.7 \pm 56.0$ ml and $\Delta ESV = -13.2 \pm 48.1$ ml) compared with controls ($\Delta EDV = -0.2 \pm 26.1$ ml and $\Delta ESV = -8.9 \pm 18.7$ ml, $p = 0.636$ and $p = 0.913$, respectively) at 1 year. No differences in the change of cardiac output or stroke volume from baseline to 1 year were detected in treated patients compared with control patients (Table 2).

Predictors of efficacy. We performed covariate analysis to investigate predictors of regenerative efficacy in CDC-treated patients at 1 year. Higher baseline scar size was strongly associated with greater scar size reduction 1 year after cell infusion ($r = -0.890$, $p < 0.001$) (Fig. 5A, Online Fig. 4A). A weak correlation between scar size reduction and baseline EF was observed ($r = 0.588$, $p = 0.044$) (Fig. 5B, Online Fig. 4B). However, when multiple linear regression analysis (using scar size treatment effect as the dependent variable and baseline EF and baseline scar size as independent variables) was performed, only baseline scar size ($p = 0.002$), but not baseline EF ($p = 0.868$), was associated with regenerative efficacy. Scar size treatment effect did not correlate with the time from MI to CDC infusion (Fig. 5C, Online Fig. 4C). Scar size reduction was similar in patients with a history of a temporally remote MI ($-12.0 \pm 4.4\%$) and patients without a previous MI ($-10.6 \pm 4.9\%$, $p = 0.649$ between groups) (Fig. 5D, Online Fig. 4D).

Discussion

The ultimate goal of cell therapy is to achieve myocardial regeneration. From the first principles, genuine regeneration should be manifested by regrowth of new functional heart muscle. Despite more than a decade of clinical trials of cell therapy, this goal remains largely elusive. In the 6-month data from the prospective, randomized, controlled CADUCEUS trial (10), we demonstrated that intracoronary infusion of autologous CDCs post-MI is feasible and appears to be safe and effective in decreasing scar size and increasing viable myocardium. The present study investigated the longevity of these effects at 1 year after cell administration; the results were only partially available at the time of the initial report.

Final 1-year data from CADUCEUS show that intracoronary administration of autologous CDCs in patients with convalescent MI did not raise significant safety concerns. The frequency of mild TnI increases (2 of 17) after CDC infusion falls within the range associated with elective angioplasty (5% to 30%) (34). Because there was no placebo control group, we cannot assess with certainty whether the cells were culpable or whether the mild TnI elevations were

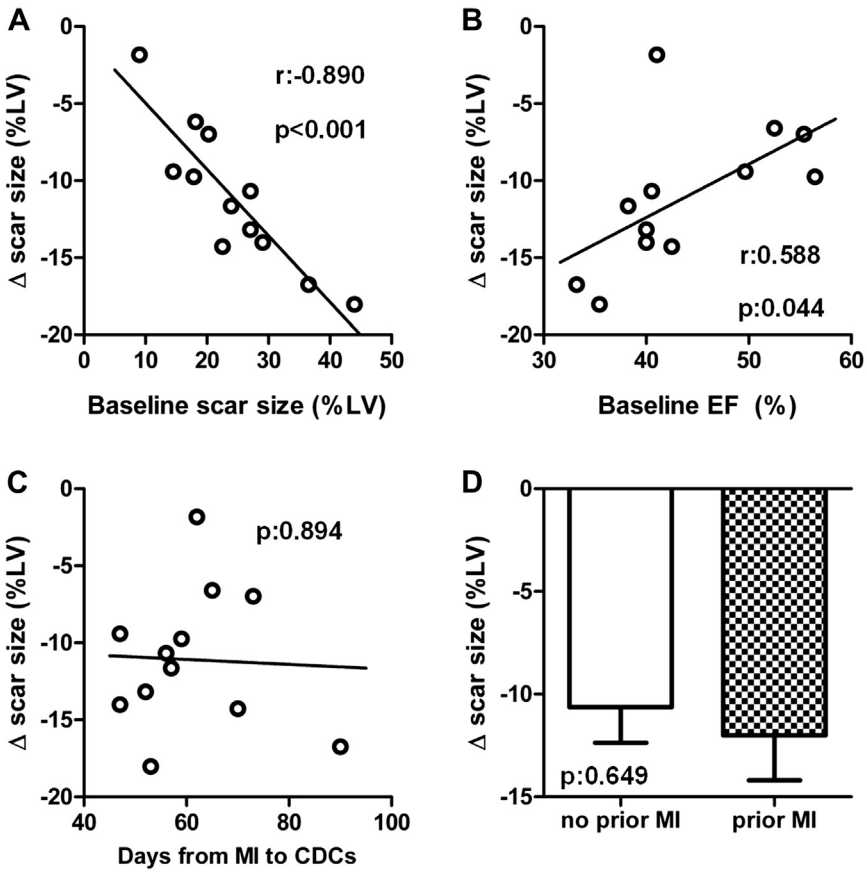

Figure 5 Predictors of Efficacy

(A) Correlation between the change in scar size (from baseline to 1 year) and baseline scar size. **(B)** Correlation between the change in scar size (from baseline to 1 year) and baseline left ventricular ejection fraction. **(C)** Correlation between the change in scar size (from baseline to 1 year) and time from MI to infusion of CDCs. **(D)** Changes in scar size from baseline to in year in CDC-treated patients with and without history of temporally remote myocardial infarction (MI). Abbreviations as in Figures 1 and 4.

due simply to the transient vessel occlusion. It also needs to be acknowledged that numerically higher rates of non-sustained ventricular tachycardias and SAEs were recorded in CDC-treated patients; the frequency of adverse events should be examined further in future trials.

Although the primary endpoints of the study were safety-related, we observed intriguing hints of efficacy. Autologous CDCs decreased scar size and improved regional function of infarcted myocardium (both were pre-specified exploratory secondary efficacy endpoints). Importantly, the correlation of scar shrinkage with the increase in viability and improvement in regional function is consistent with genuine therapeutic regeneration.

Despite the improvements in scar size and regional function, no improvements in global function were detected. Although the changes in LVEF in CDC-treated subjects were consistent with the natural relationship between scar size and EF in convalescent MI, we also observed an increase in LVEF in control patients (without any significant changes in scar measures) that falls within the margins of variability. Given the multiplicity of factors that influence EF (but not scar size, which is a structural parameter [35]) and the much higher precision of MRI for measuring scar size compared with EF (21,36), we expect that larger studies will be required to ascertain genuine changes in global function in CDC-treated patients (and in control patients). In addition, we did not detect any improvements in NYHA functional class, peak Vo_2, distance walked in 6 min or quality of life after therapy with CDCs. However, our relatively small study provided a low statistical power environment, where comparisons between groups are often uninformative and the absence of evidence does not necessarily translate to evidence of absence. Ultimately, appropriately powered studies are required to assess functional efficacy of CDCs.

CADUCEUS is the first and only controlled study to show an increase in viable myocardium, a prerequisite for myocardial regeneration. A recent interim analysis of an ongoing phase 1, single-center clinical trial using c-Kit+ heart-derived cells (28) in surgically revascularized patients

also showed an increase in viable myocardium after cell administration (37); however, the conclusions may be undermined by methodological concerns (38).

Although cardiac MRI has been extensively validated and is considered the gold-standard imaging modality for the quantification of scarred and viable myocardium (21,39), it cannot distinguish cardiac hypertrophy from hyperplasia. However, histology data from pre-clinical studies rule out myocyte hypertrophy as a contributor to the increase in viable myocardium observed after CDC therapy and suggest instead that the increased viable myocardium in the CDC-treated hearts is a direct result of an increased number of myocytes (10,40).

Important unresolved issues in the field of cell therapy include the identification of the patient population that will benefit most from cell transplantation and the ideal time of cell administration post-MI (41). With regard to the former, we show that higher baseline scar size was associated with greater regenerative efficacy in treated patients. This finding is in agreement with previous studies: in the BOOST (BOne marrOw transfer to enhance ST-elevation infarct regeneration) trial, sustained functional improvement was observed only in patients with greater infarct transmurality (5), and in the study by Janssens et al. (3), bone marrow mononuclear cell administration led to enhanced recovery of regional function only in the most severely infarcted myocardial segments. Similar conclusions have been reached in subgroup analyses of the REPAIR-AMI (Reinfusion of Enriched Progenitor Cells and Infarct Remodeling in Acute Myocardial Infarction) (6) and REGENT (Myocardial Regeneration by Intracoronary Infusion of Selected Population of Stem Cells in Acute Myocardial Infarction) (42) trials. These findings suggest that the greatest benefits of cell therapy occur in patients with the greatest infarct-induced myocardial damage, a realization that should inform the design of future clinical trials. It is equally possible, however, that subtle changes may be more difficult to quantify in patients with smaller baseline scars. With regard to the optimal time of cell administration, regenerative efficacy of CDCs in the CADUCEUS trial did not correlate with time from MI to infusion or history of temporally remote MI. In addition, the single patient infused off-protocol 14 months post-MI responded similarly to patients infused at 1.5 to 3 months post-MI. These results suggest that CDCs may confer similar benefits in chronic ischemic cardiomyopathy, as in convalescent MI.

The CADUCEUS trial was not designed to offer mechanistic insights into how CDCs may regenerate the infarcted heart. Even though CDCs are multipotent and clonogenic, and thus satisfy conventional criteria for cardiac progenitors (43), extensive pre-clinical evidence supports the conclusion that the mechanism of benefit is indirect (24,44). Cardiospheres and CDCs decrease scar mass by exerting fibrolytic actions (45) and increase viable myocardium through recruitment of endogenous progenitors and induction of resident cardiomyocyte proliferation in the infarct border zone (40). The indirect mechanisms of action (which share similarities with growth factor–based approaches [46–48]) rely on activation of endogenous reparative and regenerative pathways rather than long-term engraftment and differentiation of transplanted cells; thus, the "stemness" of CDCs appears to be unrelated to their efficacy. If, indeed, long-term survival of transplanted cells is not required for regenerative efficacy, then allogeneic CDCs may work without immunosuppression. In agreement with this prediction, we have shown that allogeneic cardiospheres and their progeny are just as effective as syngeneic CDCs in a rat model of MI (24,45). In addition, the POSEIDON (Percutaneous Stem Cell Injection Delivery Effects on Neomyogenesis Pilot Study) study of bone marrow mesenchymal cells showed that therapy with allogeneic cells appears to be safe and at least as active as therapy with autologous mesenchymal cells (49). The safety and efficacy of allogeneic CDCs in human subjects with LV dysfunction post-MI are currently being tested in the phase 1/2 randomized, double-blind, placebo-controlled ALLSTAR trial (ALLogeneic heart STem cells to achieve myocArdial Regeneration) (50). This study not only examines allogeneic cells, but also expands the eligibility window to as long as 1 year post-MI; the results will help settle the question of whether time from index MI is a major determinant of efficacy.

Study limitations. First, 2 patients (1 treated and 1 control) were lost to follow-up and did not complete their 1 year visits. Although both subjects were alive at the 1-year endpoint, we have no other information with regard to possible adverse events occurring between 6 months and 1 year, or their functional status at 1 year. Second, even though we did observe intriguing hints of regenerative efficacy in our study, it should be emphasized that CADUCEUS was a small phase 1 study, not powered to assess efficacy in a definitive manner; thus, the encouraging indications of bioactivity merit further investigation in future trials.

Conclusions

We find that intracoronary administration of autologous CDCs did not raise statistically significant safety concerns. Analysis of exploratory efficacy endpoints revealed a decrease in scar size, an increase in viable myocardium, and improved regional function of infarcted myocardium 1 year post-treatment. These findings motivate the further exploration of CDCs in future clinical studies.

Acknowledgments

The authors thank Mohammad Aminzadeh, Cynthia Leathers, Jasminka Stegic, Michelle Domingo, Tracey Gerez, Michael Tajon, and Elayne Breton for valuable assistance with recruitment and follow-up of patients; Laura Smith for performing cardiac MRIs; Kristine Evers for MRI/CT analysis; Supurna Chowdhury and Christiane Houde for culturing CDCs; and the patients who

volunteered for this study. Raj Makkar holds the Stephen Corday, MD Chair, of the Cedars-Sinai Medical Center.

Reprint requests and correspondence: Dr. Eduardo Marbán, Cedars-Sinai Heart Institute, 8700 Beverly Boulevard, Los Angeles, California 90048. E-mail: eduardo.marban@csmc.edu.

REFERENCES

1. Ford ES, Ajani UA, Croft JB, et al. Explaining the decrease in U.S. deaths from coronary disease, 1980–2000. N Engl J Med 2007;356:2388–98.
2. White HD, Aylward PE, Huang Z, et al., VALIANT Investigators. Mortality and morbidity remain high despite captopril and/or Valsartan therapy in elderly patients with left ventricular systolic dysfunction, heart failure, or both after acute myocardial infarction: results from the Valsartan in Acute Myocardial Infarction Trial (VALIANT). Circulation 2005;112:3391–9.
3. Janssens S, Dubois C, Bogaert J, et al. Autologous bone marrow-derived stem-cell transfer in patients with ST-segment elevation myocardial infarction: double-blind, randomised controlled trial. Lancet 2006;367:113–21.
4. Lunde K, Solheim S, Aakhus S, et al. Intracoronary injection of mononuclear bone marrow cells in acute myocardial infarction. N Engl J Med 2006;355:1199–209.
5. Meyer GP, Wollert KC, Lotz J, et al. Intracoronary bone marrow cell transfer after myocardial infarction: eighteen months' follow-up data from the randomized, controlled BOOST (BOne marrOw transfer to enhance ST-elevation infarct regeneration) trial. Circulation 2006;113:1287–94.
6. Schachinger V, Erbs S, Elsasser A, et al. Intracoronary bone marrow-derived progenitor cells in acute myocardial infarction. N Engl J Med 2006;355:1210–21.
7. Hare JM, Traverse JH, Henry TD, et al. A randomized, double-blind, placebo-controlled, dose-escalation study of intravenous adult human mesenchymal stem cells (prochymal) after acute myocardial infarction. J Am Coll Cardiol 2009;54:2277–86.
8. Houtgraaf JH, den Dekker WK, van Dalen BM, et al. First experience in humans using adipose tissue-derived regenerative cells in the treatment of patients with ST-segment elevation myocardial infarction. J Am Coll Cardiol 2012;59:539–40.
9. Jeevanantham V, Butler M, Saad A, Abdel-Latif A, Zuba-Surma EK, Dawn B. Adult bone marrow cell therapy improves survival and induces long-term improvement in cardiac parameters: a systematic review and meta-analysis. Circulation 2012;126:551–68.
10. Makkar RR, Smith RR, Cheng K, et al. Intracoronary cardiosphere-derived cells for heart regeneration after myocardial infarction (CADUCEUS): a prospective, randomised phase 1 trial. Lancet 2012;379:895–904.
11. Smith RR, Barile L, Cho HC, et al. Regenerative potential of cardiosphere-derived cells expanded from percutaneous endomyocardial biopsy specimens. Circulation 2007;115:896–908.
12. Specialized Centers for Cell-based Therapy (SCCT): Sponsored by the National Heart, Lung and Blood Institute (NHLBI). Available at: http://www.sccelltherapy.net. Accessed January 23, 2013.
13. Rector TS, Cohn JN. Assessment of patient outcome with the Minnesota Living with Heart Failure questionnaire: reliability and validity during a randomized, double-blind, placebo-controlled trial of pimobendan. Pimobendan Multicenter Research Group. Am Heart J 1992;124:1017–25.
14. Slavin GS, Saranathan M. FIESTA-ET: high-resolution cardiac imaging using echo-planar steady-state free precession. Magn Reson Med 2002;48:934–41.
15. Schuleri KH, Centola M, Choi SH, et al. Multi-detector computed tomography for the evaluation of myocardial cell therapy in heart failure: a comparison with cardiac magnetic resonance imaging. J Am Coll Cardiol Imaging 2011;4:1284–93.
16. Zerhouni EA, Parish DM, Rogers WJ, Yang A, Shapiro EP. Human heart: tagging with MR imaging–a method for noninvasive assessment of myocardial motion. Radiology 1988;169:59–63.
17. Helm RH, Leclercq C, Faris OP, et al. Cardiac dyssynchrony analysis using circumferential versus longitudinal strain: implications for assessing cardiac resynchronization. Circulation 2005;111:2760–7.
18. Cerqueira MD, Weissman NJ, Dilsizian V, et al. Standardized myocardial segmentation and nomenclature for tomographic imaging of the heart. A statement for healthcare professionals from the Cardiac Imaging Committee of the Council on Clinical Cardiology of the American Heart Association. Int J Cardiovasc Imaging 2002;18:539–42.
19. Garot J, Bluemke DA, Osman NF, et al. Fast determination of regional myocardial strain fields from tagged cardiac images using harmonic phase MRI. Circulation 2000;101:981–8.
20. Simonetti OP, Kim RJ, Fieno DS, et al. An improved MR imaging technique for the visualization of myocardial infarction. Radiology 2001;218:215–23.
21. Amado LC, Gerber BL, Gupta SN, et al. Accurate and objective infarct sizing by contrast enhanced magnetic resonance imaging in a canine myocardial infarction model. J Am Coll Cardiol 2004;44:2383–9.
22. Wu E, Ortiz JT, Tejedor P, et al. Infarct size by contrast enhanced cardiac magnetic resonance is a stronger predictor of outcomes than left ventricular ejection fraction or end-systolic volume index: prospective cohort study. Heart 2008;94:730–6.
23. Johnston PV, Sasano T, Mills K, et al. Engraftment, differentiation, and functional benefits of autologous cardiosphere-derived cells in porcine ischemic cardiomyopathy. Circulation 2009;120:1075–83.
24. Malliaras K, Li TS, Luthringer D, et al. Safety and efficacy of allogeneic cell therapy in infarcted rats transplanted with mismatched cardiosphere-derived cells. Circulation 2012;125:100–12.
25. Dominici M, Le Blanc K, Mueller I, et al. Minimal criteria for defining multipotent mesenchymal stromal cells. The International Society for Cellular Therapy position statement. Cytotherapy 2006;8:315–7.
26. Pelekanos RA, Li J, Gongora M, et al. Comprehensive transcriptome and immunophenotype analysis of renal and cardiac MSC-like populations supports strong congruence with bone marrow MSC despite maintenance of distinct identities. Stem Cell Res 2012;8:58–73.
27. Ieda M, Tsuchihashi T, Ivey KN, et al. Cardiac fibroblasts regulate myocardial proliferation through beta1 integrin signaling. Dev Cell 2009;16:233–44.
28. Beltrami AP, Barlucchi L, Torella D, et al. Adult cardiac stem cells are multipotent and support myocardial regeneration. Cell 2003;114:763–76.
29. Goldsmith EC, Hoffman A, Morales MO, et al. Organization of fibroblasts in the heart. Dev Dyn 2004;230:787–94.
30. Sun Y, Weber KT. Infarct scar: a dynamic tissue. Cardiovasc Res 2000;46:250–6.
31. Albelda SM, Muller WA, Buck CA, Newman PJ. Molecular and cellular properties of PECAM-1 (endoCAM/CD31): a novel vascular cell-cell adhesion molecule. J Cell Biol 1991;114:1059–68.
32. Cheng K, Malliaras K, Li TS, et al. Magnetic enhancement of cell retention, engraftment, and functional benefit after intracoronary delivery of cardiac-derived stem cells in a rat model of ischemia/reperfusion. Cell Transplant 2012;21:1121–35.
33. Quinn J, Kramer N, McDermott D. Validation of the Social Security Death Index (SSDI): an important readily-available outcomes database for researchers. West J Emerg Med 2008;9:6–8.
34. Prasad A, Herrmann J. Myocardial infarction due to percutaneous coronary intervention. N Engl J Med 2011;364:453–64.
35. Malliaras K, Kreke M, Marbán E. The stuttering progress of cell therapy for heart disease. Clin Pharmacol Ther 2011;90:532–41.
36. Greupner J, Zimmermann E, Grohmann A, et al. Head-to-head comparison of left ventricular function assessment with 64-row computed tomography, biplane left cineventriculography, and both 2- and 3-dimensional transthoracic echocardiography: comparison with magnetic resonance imaging as the reference standard. J Am Coll Cardiol 2012;59:1897–907.
37. Chugh AR, Beache GM, Loughran JH, et al. Administration of cardiac stem cells in patients with ischemic cardiomyopathy: the SCIPIO trial: surgical aspects and interim analysis of myocardial function and viability by magnetic resonance. Circulation 2012;126 Suppl 1:S54–64.
38. Kreke M, Smith RR, Marbán L, Marbán E. Cardiospheres and cardiosphere-derived cells as therapeutic agents following myocardial infarction. Expert Rev Cardiovasc Ther 2012;10:1185–94.

39. Kim RJ, Fieno DS, Parrish TB, et al. Relationship of MRI delayed contrast enhancement to irreversible injury, infarct age, and contractile function. Circulation 1999;100:1992–2002.
40. Malliaras K, Zhang Y, Seinfeld J, et al. Cardiomyocyte proliferation and progenitor cell recruitment underlie therapeutic regeneration after myocardial infarction in the adult mouse heart. EMBO Mol Med 2013;5:191–209.
41. Malliaras K, Marbán E. Cardiac cell therapy: where we've been, where we are, and where we should be headed. Br Med Bull 2011;98:161–85.
42. Tendera M, Wojakowski W, Ruzyllo W, et al. Intracoronary infusion of bone marrow-derived selected CD34+CXCR4+ cells and non-selected mononuclear cells in patients with acute STEMI and reduced left ventricular ejection fraction: results of randomized, multicentre Myocardial Regeneration by Intracoronary Infusion of Selected Population of Stem Cells in Acute Myocardial Infarction (REGENT) Trial. Eur Heart J 2009;30:1313–21.
43. Davis DR, Ruckdeschel Smith R, Marbán E. Human cardiospheres are a source of stem cells with cardiomyogenic potential. Stem Cells 2010; 28:903–4.
44. Chimenti I, Smith RR, Li TS, et al. Relative roles of direct regeneration versus paracrine effects of human cardiosphere-derived cells transplanted into infarcted mice. Circ Res 2010;106:971–80.
45. Tseliou E, Pollan S, Malliaras K, et al. Allogeneic cardiospheres safely boost cardiac function and attenuate adverse remodeling after myocardial infarction in immunologically mismatched rat strains. J Am Coll Cardiol 2013;61:1108–19.
46. Penn MS, Mendelsohn FO, Schaer GL, et al. An open-label dose escalation study to evaluate the safety of administration of nonviral stromal cell-derived factor-1 plasmid to treat symptomatic ischemic heart failure. Circ Res 2013;112:816–25.
47. Yaniz-Galende E, Chen J, Chemaly E, et al. Stem cell factor gene transfer promotes cardiac repair after myocardial infarction via in situ recruitment and expansion of c-kit+ cells. Circ Res 2012;111: 1434–45.
48. Segers VF, Tokunou T, Higgins LJ, MacGillivray C, Gannon J, Lee RT. Local delivery of protease-resistant stromal cell derived factor-1 for stem cell recruitment after myocardial infarction. Circulation 2007;116:1683–92.
49. Hare JM, Fishman JE, Gerstenblith G, et al. Comparison of allogeneic vs autologous bone marrow–derived mesenchymal stem cells delivered by transendocardial injection in patients with ischemic cardiomyopathy: the POSEIDON randomized trial. JAMA 2012;308:2369–79.
50. Allogeneic Heart Stem Cells to Achieve Myocardial Regeneration (ALLSTAR) (NCT01458405). Available at: http://clinicaltrials.gov/ct2/show/NCT01458405?term=allstar&rank=1. Accessed January 13, 2013.

Key Words: cardiosphere-derived cells ■ myocardial infarction ■ myocardial regeneration.

APPENDIX

For supplemental tables, figures, and videos and their legends, please see the online version of this article.